

## Producing $\mu\text{Bq}/\text{m}^3$ level low $^{226}\text{Ra}$ ultrapure water for the Jiangmen Underground Neutrino Observatory

**Authors:** Xu, Mr. Xiting, Guo, Dr. Cong, Liu, Prof. Jinchang, Zhang, Dr. Yongpeng, Liang, Dr. Xiaohua, WEN, Xin-Jian, Yang, Prof. Changgen, TANG, Prof. Quan, Lv, Mrs. Lidan, Niu, Mr. Yuanhao, Xiao, Mr. Bin, Guo, Dr. Cong

**Date:** 2026-03-27T23:21:41+00:00

### Abstract

The Jiangmen Underground Neutrino Observatory (JUNO), a 20~ktons low-background Liquid Scintillator (LS) detector, was primarily designed to determine the neutrino mass ordering. JUNO requires UltraPure Water (UPW) with a  $^{226}\text{Ra}$  concentration  $\leq 50 \text{ Bq}/\text{m}^3$  due to the direct liquid-liquid contact between LS and UPW during detector filling. To meet this stringent requirement, a highly sensitive measurement system capable of detecting  $3.9\text{-}\mu\text{Bq}/\text{m}^3$  of  $^{226}\text{Ra}$  was developed, and the 100~t/h UPW production process was optimized. By integrating selective ion-exchange resin with membrane separation technologies, UPW with a  $^{226}\text{Ra}$  concentration of  $\leq 4 \text{ Bq}/\text{m}^3$  was consistently produced, exceeding JUNO's specifications and setting a world-leading benchmark. This paper describes the design and implementation of JUNO's UPW system and the highly sensitive  $^{226}\text{Ra}$  measurement system, along with a systematic evaluation of  $^{226}\text{Ra}$  removal efficiency across purification stages and final water quality validation.

### Full Text

#### Preamble

Producing  $\mu\text{Bq}/\text{m}^3$  level low  $^{226}\text{Ra}$  ultrapure water for the Jiangmen Underground Neutrino Observatory\* Xi-Ting Xu,<sup>1</sup> Cong Guo,<sup>2, 3, 4</sup> † Jin-Chang Liu,<sup>2, 3, 4</sup> Yong-Peng Zhang,<sup>2, 3, 4</sup> Xiao-Hua Liang,<sup>5</sup> Xin-Jian Wen,<sup>1</sup> ‡ Chang-Gen Yang,<sup>2, 3, 4</sup> Quan Tang,<sup>6</sup> § Li-Dan Lv,<sup>6</sup> Yuan-Hao Niu,<sup>1</sup> and Bin Xiao<sup>7</sup>

Institute of Theoretical Physics, Shanxi University, Taiyuan, 030006, China Experimental Physics Division, Institute of High Energy Physics, Chinese Academy

of Sciences, Beijing, 100049, China School of Physics, University of Chinese Academy of Sciences, Beijing, 100049, China State Key Laboratory of Particle Detection and Electronics, Beijing, 100049, China Astro-particle Physics Division, Institute of High Energy Physics, Chinese Academy of Sciences, Beijing, 100049, China School of Nuclear Science and Technology, University of South China, Hengyang, 421001, China School of Mechanics and Optoelectronic Physics, Anhui University of Science and Technology, Huainan, 232001, China The Jiangmen Underground Neutrino Observatory (JUNO), a 20 ktons low-background Liquid Scintillator (LS) detector, was primarily designed to determine the neutrino mass ordering. JUNO requires UltraPure Water (UPW) with a  $^{226}\text{Ra}$  concentration  $<50\ \mu\text{Bq}/\text{m}^3$  due to the direct liquid-liquid contact between LS and UPW during detector filling. To meet this stringent requirement, a highly sensitive measurement system capable of detecting  $3.9\ \mu\text{Bq}/\text{m}^3$  of  $^{226}\text{Ra}$  was developed, and the 100 t/h UPW production process was optimized. By integrating selective ion-exchange resin with membrane separation technologies, UPW with a  $^{226}\text{Ra}$  concentration of  $<4\ \mu\text{Bq}/\text{m}^3$  was consistently produced, exceeding JUNO's specifications and setting a world-leading benchmark. This paper describes the design and implementation of JUNO's UPW system and the highly sensitive Ra measurement system, along with a systematic evaluation of  $^{226}\text{Ra}$  removal efficiency across purification stages and final water quality validation.

## Keywords

JUNO, Ultra Pure Water,  $^{226}\text{Ra}$ , Reverse Osmosis, Resin

## INTRODUCTION

Cherenkov Detector (WCD), and a Top Tracker (TT) detector. The CD contains 20 ktons of ultrapure LS housed in a 25 spherical acrylic vessel and is submerged in the WCD, which holds 40 ktons of Ultra Pure Water (UPW) and is instrumented with 2400 20-inch MicroChannel Plate Photomultiplier Tubes (MCP-PMTs). The WCD provides sufficient water shielding to protect the CD from ambient radioactivity and simultaneously serves as a cosmic muon veto. For background and safety reasons, the CD and WCD must be initially filled simultaneously with UPW. Subsequently, the UPW in the CD is replaced with LS at a production rate of 7 m<sup>3</sup>/h. During this replacement process, UPW and LS come into direct contact. As this stage marks the final step before detector operation, strict control of radionuclides in the water is critical to prevent contamination of the LS by the UPW. One of the most challenging requirements is to maintain the concentration in the water to below  $50\ \mu\text{Bq}/\text{m}^3$  [2].

The Jiangmen Underground Neutrino Observatory (JUNO) [1-4] is a multipurpose experiment designed primarily to determine the neutrino mass ordering and to precisely measure neutrino oscillation parameters by detecting reactor

6 antineutrinos.

With 20 kt of low-background Liquid Scintillator (LS) and an unprecedented energy resolution of 8.3%@1MeV, JUNO is the largest LS-based underground neutrino observatory, capable of addressing numerous important topics in astroparticle physics.

JUNO's extensive physics program encompasses supernova neutrinos, atmospheric neutrinos, solar neutrinos, geoneutrinos, and searches for new physics [1, 2]. Located in an underground laboratory with 700 m overburden, the muon flux at the JUNO site is about 4 mHz/m with a mean energy of 207 GeV [5]. The primary detection channel for reactor antineutrinos in JUNO is the inverse beta decay reaction on protons. JUNO is expected to detect only 60 reactor antineutrino events per day, making stringent control of radioactive backgrounds essential [6].

In the field of low-background water purification and  $^{226}\text{Ra}$  detection, the Sudbury Neutrino Observatory (SNO) [7] and Super-Kamiokande (Super-K) [8] experiments have achieved internationally recognized advances. SNO developed a measurement technique using manganese oxide-coated beads, achieving a  $^{226}\text{Ra}$  detection sensitivity of  $10 \mu\text{Bq}/\text{m}^3$ . The initial  $^{226}\text{Ra}$  concentration in SNO's UPW was  $50 \mu\text{Bq}/\text{m}^3$ , which was later reduced to  $10\text{--}20 \mu\text{Bq}/\text{m}^3$  through recirculation and purification [9]. Super-K adopted SNO's method and attained a similar sensitivity of  $10 \mu\text{Bq}/\text{m}^3$ , although its UPW exhibited slightly higher  $^{226}\text{Ra}$  levels, with (Grant No. 2023015). † Corresponding author, C. Guo, E-mail address: guocong@ihep.ac.cn initial concentration of  $61 \pm 13 \mu\text{Bq}/\text{m}^3$ , decreasing to  $32 \pm 7 \mu\text{Bq}/\text{m}^3$  after recirculation [10]. In terms of production § Corresponding author, Q. Tang, E-mail address: tanquan528@sina.com 53 scale, Super-K's water system has a capacity of 30 t/h [10],

substantially larger than SNO's 9 t/h system [7].

#### UPW SYSTEM

The JUNO experiment employs a 100 t/h UPW system to provide 40 kt of UPW for the WCD. This system produces ultrapure water that meets the following specifications: a resistivity  $>18.2 \text{ M}\Omega\cdot\text{cm}$ , a  $^{226}\text{Ra}$  concentration of  $<1 \times 10^4 \mu\text{Bq}/\text{m}^3$ ,  $^{232}\text{Th}$  concentration of  $<4 \mu\text{Bq}/\text{m}^3$ ,  $^{235}\text{U}$  concentration of  $<4 \mu\text{Bq}/\text{m}^3$ , and a minimum temperature of 17°C, thereby ensuring high passing both the JUNO requirement and the performance of muon detection efficiency for the WCD, negligible radioactive comparable experiments. To achieve such ultra-low detection contribution to the CD, and thermal stability for the 60 t/h system, we developed a high-sensitivity measurement system [1]. In addition, for the initial filling of the acrylic

vessel, based on Mn-fiber adsorption and radon emanation, reaching this system must deliver UPW at 50 t/h with a Ra concentration sensitivity of 3.9  $\mu\text{Bq}/\text{m}^3$  through optimized Mn-fiber synthesis below 50  $\mu\text{Bq}/\text{m}^3$  [2]. The system operates reliably at 100 t/h, demonstrating the JUNO 100 t/h UPW system utilizes tap water as feedwater, proving its feasibility for large-scale engineering. Furthermore, the system produces UPW that is compliant with China's national standard through systematic optimization and pollution source tracing, meeting electronic grade EW-I standard [11].

As shown in Fig. 2 [Figure 2: see original paper], we identified the softening resin and reverse osmosis membrane as the key removal components (both achieving >99% radium removal efficiency), and pinpointed the primary contamination sources as sediment and sea salt. Bag filters (with a pore size of 5  $\mu\text{m}$ ) and air ingress via the tank breather valve, enabling targeted - Multi-media filters (with stratified quartz sand, activated carbon, and anthracite). - Activated carbon filters (using coconut shell-derived carbon).

This paper is structured as follows. Sec. II describes the Softening resin columns (with special resin from Jiangsu Suqing Water Treatment Engineering UPW system of the WCD). Sec. III details the 3.9  $\mu\text{Bq}/\text{m}^3$  highly sensitive Ra in water measurement system. The measurement results of the Ra concentrations after each Cartridge filters (with a pore size of 5  $\mu\text{m}$ ). - Reverse Osmosis (RO) membranes. purification stage and in the final product water are presented in Sec. IV. Potential upgrades to the system for enhanced Ra removal are discussed in Sec. V, and a summary of using bag filters for bulk particulate removal, followed by multi-media filtration for the reduction of suspended solids.

Subsequent activated carbon adsorption removes residual diatoms while oxidatively decomposing organics. Degassing chlorine, organic compounds, ammonia-nitrogen species, membranes, which employ hollow fibers, vacuum pumps, and tritium, trace heavy metals, and microbial contaminants. The purging nitrogen, remove dissolved gases via partial pressure ion-exchange softening process achieves Ca<sup>2+</sup>/Mg<sup>2+</sup> removal and are critical for the removal of Rn from water through cationic substitution. After intermediate storage [14-16]. The microbubble generator enhances the water age, water passes through cartridge filters (5  $\mu\text{m}$ ) to improve removal efficiency of the degassing membranes by reloading downstream equipment. The RO array provides primary nitrogen into the water [14, 16]. Heat exchangers regulate desalination via semipermeable membranes, achieving near-ambient temperature. UF membranes (with a pore size of <10 nm) remove trace amounts of ions, particles, colloids, and

bacteria 118 complete ionic rejection [12].

The multi-media filters, activated carbon units, and softening resins are regenerable. Multi-media filters and activated carbon units undergo hydraulic backwashing to restore capacity and the initial filling of the CD. Owing to their distinct requirements, the two streams undergo separate treatments. The CD-bound water, which contacts the LS directly, receives additional UF for enhanced removal of ionic contaminants. The product water from the aboveground system is transferred underground through a 1,300 m stainless-steel pipeline. With an elevation differential of 450 m, the water first passes through a pressure-reducing valve before entering the detector storage tank. The underground water system comprises the following components: - Secondary RO membranes (for enhanced desalination). - Electrodeionization (EDI) device. - Cartridge filters (with a pore size of 0.1  $\mu\text{m}$ ). - Total Organic Carbon (TOC) removal. - Ultraviolet (UV) sterilization. - Degassing membranes.

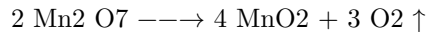
MEASUREMENT - Microbubble generator. - Heat exchangers. - Ultra-Filtration (UF).

The required concentration of  $50 \mu\text{Bq}/\text{m}^3$  ( $2 \times 10^{-21} \text{ g}/\text{g}$ ) is beyond the detection capability of conventional methods like high-purity germanium spectrometry [17] and resin under a DC field for continuous deionization without inductively coupled plasma mass spectrometry [18]. There chemical regeneration [13]. Cartridge filters capture residual radon, a custom system was developed that determines the radon activity by measuring its gaseous daughter, radon particles. The TOC/UV systems sterilize through UV irradiation.

of the key adsorbent, the Mn-fiber, from  $17 \mu\text{Bq}/\text{g}$  to  $10.7 \pm 1.5 \mu\text{Bq}/\text{g}$ . This was achieved through three major enhancements to the standard synthesis protocol [21, 22]:

The initial step in measuring the Ra concentration in water via Rn emanation is Ra preconcentration. (1) Nitric acid pre-cleaning of the polyurethane fibers. This method leverages the strong adsorption of Ra onto MnO<sub>2</sub> [9, 19, 20] by using laboratory-synthesized Manganese fiber (Mn-fiber) [21, 22]. (3) Substituting distilled water with high-purity water from China Resources Beverage (China) Co., Ltd for rinsing—the most impactful change.

Measurement principle



parentheses are the half-lives. The energies shown for  $\alpha$  decay are peak energies, while those for  $\beta$  decay are the maximum energies.

Following  $^{226}\text{Ra}$  extraction, the activity of  $^{222}\text{Rn}$  emanated from the Mn-fiber during a sealed period is measured. Fig. 3 [Figure 3: see original paper] illustrates the relevant decay branch of Ra. During sealing, the relationship between the activity of Ra and its  $^{222}\text{Rn}$  progeny activity can be calculated using Eq. 1 [21]:

$$A_{\text{Rn}}(t) = A_{\text{Ra}} \times (e^{-\lambda_{\text{Ra}} t} - e^{-\lambda_{\text{Rn}} t}) / (\lambda_{\text{Rn}} - \lambda_{\text{Ra}})$$

where  $A_{\text{Rn}}(t)$  is the  $^{222}\text{Rn}$  activity at time  $t$  in mBq,  $A_{\text{Ra}}$  is the initial Ra activity extracted by Mn-fiber in mBq,  $\lambda_{\text{Rn}}$  is the decay constant of Rn,  $\lambda_{\text{Ra}}$  is the decay constant of Ra. The Mn-fiber itself is produced by creating a firm  $\text{MnO}_2$  coating on the polyurethane fibers via the reaction of  $\text{KMnO}_4$  and  $\text{H}_2 \text{SO}_4$ , and  $t$  is the Mn-fiber sealing time in days.

Given that the half-life of  $^{226}\text{Ra}$  is significantly longer than that of  $^{222}\text{Rn}$  (i.e.,  $\lambda_{\text{Ra}} \ll \lambda_{\text{Rn}}$ ), Eq. 1 can be simplified to  $A_{\text{Rn}}(t) \approx A_{\text{Ra}}(1 - e^{-\lambda_{\text{Rn}} t})$ . The activity of the Mn-fiber is shown in Fig. 4 [Figure 4: see original paper]. Gravimetric analysis indicates a 13% mass increase in polyurethane fibers after

## 190 Eq. 2:

$$A_{\text{Rn}}(t) / A_{\text{Ra}} = 1 - e^{-\lambda_{\text{Rn}} t}$$

Extraction column

Measurement procedures and devices

The  $^{226}\text{Ra}$  extraction column, illustrated in Fig. 5 [Figure 5: see original paper], is constructed from an acrylic tube (20 mm inner diameter and 185 mm long) sealed with rubber gaskets and 10 mm quick connects. The assembled unit withstands water pressures up to 5 kg/cm<sup>2</sup>. Approximately 5 g of Mn-fiber is packed in the central section, flanked by polyurethane fibers at both ends to filter particulate matter. During operation, water is directed

## 1. Mn-fiber

226 upward through the column to maximize contact with the Mn-227 fiber. A residential water meter (GB/T 778 compliant [23], To meet JUNO's requirement for  $\mu\text{Bq}/\text{m}^3$  -level 226 Ra mea- 228  $\pm 2\%$  accuracy) at the outlet measures the total volume of wa-226 199 surements, we significantly reduced the Ra background 229 ter passed through the Mn-fiber.

- (2) Mn-fiber container. Two chamber types are used (Fig. 7 [Figure 7: see original paper]): a standard CF35 tube (150 mm long) for 5 g 263 samples, and a custom chamber (130 mm diameter and 264 300 mm length) for <300 g samples for background mea-265 surement. All inner surfaces were electropolished to a rough-266 ness of  $<0.1 \mu\text{m}$ . After loading, chambers are purged with 267 boil-off nitrogen to remove residual air and then sealed for 268 several days to allow Rn ingrowth. The activity ratio be-226 269 tween Ra and Rn can be calculated using Eq. 2. For in-222 270 stance, after a 10-day sealing interval, Rn activity reaches 271 83.7% of the initial Ra activity. (3) Dehumidification systems. Mn-fibers that have extracted Ra retain substantial water, releasing significant water va-274 por during radon transfer that degrades detector efficiency 275 through humidity interference. This system comprises a liq-276 uid nitrogen tank, a solenoid valve, a dewar, a PT100 tem-277 perature sensor, and a temperature controller. Through the 278 thermostatic regulation of intermittent liquid nitrogen injec-279 tion into the dewar, the system maintains a temperature of 280  $-60 \text{ C}$  inside the dewar, reducing the relative humidity to 3% 281 at a 1 L/min gas flow rate without introducing background. (4) MFC. The MFC is used to regulate the gas flow rate 283 during radon transfer operations, with an adjustment range of 284 0.5-5 L/min. 222 Rn emanation measurement system (5) Vacuum pump. Before measurements, the pump evac-286 uates the radon detector and associated pipelines.

Subse-231 The 226 Ra activity extracted by Mn-fibers was quantified 287 quently, boil-off nitrogen is used to purge the emanated 232 by measuring its gaseous daughter Rn using a radon ema-288 from the Mn-fiber container into the radon detector. 233 nation measurement system (Fig. 6 [Figure 6: see original paper]). The system comprises a (6) Pipelines and valves. All stainless steel gas pipelines 234 radon detector, a Mn-fiber container, a dehumidification sys-290 and interconnecting valves are EP-grade components. 235 tem, a mass flow controller (MFC, Model 1179A, MKS), and

a vacuum pump (Model ACP40, Pfeiffer Vacuum). All connections use metal-sealed ConFlat flanges and VCR compo-9 238 nents, ensuring a leak tightness  $<1 \times 10^{-9} \text{ Pa}\cdot\text{m}^3/\text{s}$ . Key 291 C. Extraction efficiency calibration 239 components are summarized below; full details were de-240 scribed in our previous work [22].

The efficiency of extracting 226 Ra from water with Mn-241 (1) Radon detector. The radon detector operates on the 293 fiber was calibrated using a standardized 226 Ra solution with 242 principle of electrostatic collection [24-30], where

the de<sup>3</sup> <sup>294</sup> a concentration of  $(9.04 \pm 0.53) \times 10 \mu\text{Bq}/\text{m}^3$ . Our prior <sup>243</sup> tecton efficiency for radon progeny correlates with applied <sup>295</sup> work [22] shows consistent extraction efficiency across <sup>244</sup> collection voltage and gas humidity. At 3% relative humid<sup>4</sup> <sup>296</sup> concentrations ( $760\text{--}6.1 \times 10 \mu\text{Bq}/\text{m}^3$ ) and water flow rates <sup>245</sup> ity and  $-700 \text{ V}$  collection voltage, the detector achieves 90% <sup>297</sup> ( $1.6\text{--}8 \text{ L}/\text{min}$ ). To cover Ra concentrations from 1 to 1 <sup>246</sup> collection efficiency for Rn progeny <sup>214</sup> Po. This corre- <sup>298</sup>  $\times 104 \mu\text{Bq}/\text{m}^3$  in JUNO, sample volumes are varied, which <sup>247</sup> sponds to a calibration factor (CF) of  $67 \pm 6.7$  counts per <sup>299</sup> requires dedicated calibration of the extraction efficiency for <sup>248</sup> hour per Bq/m (cph/(Bq/m)). The system's single-day mea<sup>300</sup> different volumes. In contrast to absolute quantification, we <sup>249</sup> surement sensitivity is  $0.7 \text{ mBq}/\text{m}$  for Rn [24]. For each <sup>301</sup> employed a relative scheme with volume-matched control ex<sup>250</sup> sample measurement, the radon detector integrates radon ac<sup>302</sup> periments to simultaneously mitigate detector systematic un<sup>251</sup> tivity over a 24-hour data-taking period. As the measured <sup>303</sup> certainties and background in this work. <sup>252</sup> value represents the average Rn concentration during this Tab. 1 presents the calibrated <sup>226</sup> Ra extraction efficiencies <sup>253</sup> interval, determination of the initial Rn concentration re<sup>305</sup> across different water volumes. Throughout the test, an addi<sup>254</sup> quires correction for radioactive decay, which can be calcu<sup>226</sup> <sup>306</sup> tional  $150 \mu\text{L}$  of Ra solution was added per  $300 \text{ L}$  of water, <sup>255</sup> lated using Eq. 5 [22]: <sup>307</sup> and the water flow rate through the Mn-fiber was maintained <sup>308</sup> at  $5 \text{ L}/\text{min}$ .

$A_{\text{Rn}} - M \times \lambda_{\text{Rn}} \times (t_2 - t_1) A_{\text{Rn}} = (5)$  <sup>309</sup> For water volumes below  $1 \text{ m}^3$  passing through the Mn- $\lambda$  <sup>310</sup> fiber extraction column, Ra extraction efficiency ap<sup>222</sup> <sup>257</sup> where  $A_{\text{Rn}}$  is the initial Rn activity after transfer into the <sup>311</sup> proached 100%. Beyond this volume, a progressive decline <sup>258</sup> detector in mBq,  $A_{\text{Rn}} - M$  is the measured Rn activity in <sup>312</sup> in <sup>226</sup> Ra adsorption efficiency was observed, which might be Ra being shed from <sup>259</sup> mBq,  $t_1$  is the measurement start time in hours, and  $t_2$  is the <sup>313</sup> caused by a small amount of adsorbed <sup>314</sup> the MnO<sub>2</sub> coating. <sup>260</sup> measurement end time in hours.

<sup>226</sup> Ra extraction efficiencies of Mn-fiber for different water volumes. The uncertainties in UPW volume are derived from the accuracy of the water flow meter. The statistical uncertainties in efficiency are based on Poisson statistics, while the systematic uncertainties are determined by the uncertainty in the activity of the radium solution. For samples No. 1-No. 4, the radon detector data-taking time was 24 h, whereas for samples No. 5 and No. 6, it was 15 h.

No. UPW volume ( $\text{m}^3$ )

Ra extraction efficiency (%)

$0.3 \pm 0.006$

$99.0 \pm 13.8_{\text{stat}} \pm 5.8_{\text{sys}}$

$0.5 \pm 0.01$

$98.5 \pm 10.6_{\text{stat}} \pm 5.8_{\text{sys}}$

$1.0 \pm 0.02$  $99.5 \pm 7.6_{\text{stat}} \pm 5.8_{\text{sys}}$  $5.0 \pm 0.1$  $94.6 \pm 3.3_{\text{stat}} \pm 5.5_{\text{sys}}$  $10.0 \pm 0.2$  $91.3 \pm 2.9_{\text{stat}} \pm 5.4_{\text{sys}}$  $20.0 \pm 0.4$  $89.2 \pm 2.0_{\text{stat}} \pm 5.2_{\text{sys}}$ 

Sensitivity estimation

background event rate The sensitivity of measuring  $^{226}\text{Ra}$  concentration in wa-  
 $^{226}\text{Ra}$  lation assumes a normally distributed  $^{222}\text{Rn}$  and radioactive equilibrium  
between  $^{222}\text{Rn}$  and  $^{226}\text{Ra}$ .  $^{222}\text{Rn}$  ter at a 95% confidence level can be estimated  
according to The system background was determined by measuring 5 g

**318 Eq. 6 [29]:**

329 of unused Mn-fiber following the standard sealing and anal330 ysis proce-  
dure. Ten replicate measurements yielded a mean  $1.645 \times \sigma_{\text{BG}} \times V_{\text{s}}$  (6)  
331 background of 2.7 CPD (Fig. 8 [Figure 8: see original paper]), reflecting  
contributions from  $24 \times \text{CF} \times V_{\text{w}} \times \epsilon \times 10$  332 both the apparatus and the  
Mn-fiber.

Using the parameters described above and calculated with 320 where L is the  
sensitivity in  $\mu\text{Bq}/\text{m}$ ,  $\sigma_{\text{BG}}$  is the statistical 333 321 uncertainty of the system'  
s background event rate in Counts 334 Eq. 6, a sensitivity of 3.9  $\mu\text{Bq}/\text{m}$  for Ra  
concentration in of wa322 Per Day (CPD),  $V_{\text{s}} = 0.042$  m is the total volume of  
the mea- 335 water was derived. This calculation assumes 20 m 323 surement  
system,  $\text{CF} = 67 \pm 6.7$  cph/(Bq/m) is the detector 336 ter passes through 5  
g Mn-fiber with a Ra extraction effi3  $^{222}\text{Rn}$  activity 324 calibration factor,  $V_{\text{w}}$  is  
the sample water volume in m, and  $\epsilon$  337 ciency of 89.2%, and the data-taking  
time for 325 is the Ra extraction efficiency listed in Tab. 1. This calcu- 338  
measurement is 24 h.

counter), and resistivity (using an AZ8302 portable meter and a +GF+ Signet  
9900 in-line meter) were conducted across the 100 t/h UPW system. Uncer-  
tainties are reported as follows: for  $^{226}\text{Ra}$  concentration, the statistical un-  
certainties are based on Poisson statistics, while the systematic uncertainties  
include contributions from the calibration factor, water volume, and  $^{226}\text{Ra}$   
extraction efficiency; for particulate matter count, uncertainties are statistical  
only; and for resistivity, uncertainties correspond to the instrument display ac-  
curacy. Missing resistivity values are due to meter limitations at high resistivity  
ranges. The large relative uncertainty at S17 for the particulate matter arises

from counting statistics: each measurement used a 20 mL sample, yielding an average of 2 counts per 20 mL, which converts to  $100 \pm 70$  counts/L based on Poisson uncertainty ( $\sqrt{2} \times 50$ ). For sampling locations, refer to Fig. 2.

Ra concentration

Particulate matter  $> 0.5 \mu\text{m}$

Resistivity

(Counts/L)

( $\text{M}\Omega \cdot \text{cm}$ )

$(429 \pm 4_{\text{stat}} \pm 68_{\text{sys}}) \times 10$

$601150 \pm 5482$

$0.019 \pm 0.001$

$(186 \pm 3_{\text{stat}} \pm 29_{\text{sys}}) \times 10$

$298750 \pm 3864$

$0.019 \pm 0.001$

$(194 \pm 3_{\text{stat}} \pm 31_{\text{sys}}) \times 10$

$341850 \pm 4134$

$0.019 \pm 0.001$

$(147 \pm 2_{\text{stat}} \pm 23_{\text{sys}}) \times 10$

$17650 \pm 939$

$0.019 \pm 0.001$

$(426 \pm 4_{\text{stat}} \pm 67_{\text{sys}}) \times 10$

$22500 \pm 1060$

$0.018 \pm 0.001$

$504 \pm 114_{\text{stat}} \pm 71_{\text{sys}}$

$46600 \pm 1526$

$0.018 \pm 0.001$

$(76 \pm 1_{\text{stat}} \pm 11_{\text{sys}}) \times 10$

$341850 \pm 4134$

$0.018 \pm 0.001$

$(55 \pm 1_{\text{stat}} \pm 8_{\text{sys}}) \times 10$

$244900 \pm 3499$

0.052 ± 0.001  
79 ± 24stat ± 9sys  
2150 ± 328  
0.190 ± 0.002  
(15.8 ± 0.6stat ± 2.2sys ) × 10  
10050 ± 709  
0.470 ± 0.005  
84 ± 25stat ± 17sys  
2750 ± 370  
96 ± 26stat ± 12sys  
2250 ± 335  
56 ± 21stat ± 7sys  
2150 ± 327  
17.74 ± 0.01  
49 ± 22stat ± 6sys  
900 ± 200  
6.3 ± 4.5stat ± 0.7sys  
850 ± 206  
18.19 ± 0.01  
19.4 ± 5.8stat ± 2.2sys  
350 ± 132  
100 ± 70  
18.20 ± 0.01  
Counts  
( $\mu\text{Bq/m}$  )  
Location

## RESULTS

Entries Std Dev

Ra concentrations across the system

Using the custom-developed device described above, the Ra concentrations in water at different locations of the 343 JUNO 100 t/h UPW system, marked as S1–S17 in Fig. 2, 344 were measured, and the results are shown in Tab. 2. The water 345 volume used for S1–S5 was 0.5 m<sup>3</sup>, for S6–S8 and S10 was 346 1 m<sup>3</sup>, for S9 and S11–S14 was 5 m<sup>3</sup>, and for S15–S17 was 347 20 m<sup>3</sup>. All measurements were performed after a 10-day MnO<sub>2</sub> 348 fiber sealing period and a 24-hour Rn counting interval.

Background/CPD 349 Reported uncertainties include both statistical and systematic 350 contributions. During the 45-day filling campaign, a total of ground measurement, the Mn-fiber was sealed for 10 days. The un- 352 measurement results were below the detector's average backscatter on the Y-axis are statistical only. 353 ground; therefore, only an upper limit is provided.

In low-salinity solutions, 226 Ra exists predominantly as un<sup>2+</sup> 355 complexed Ra [31–33], making it removable via deioniza<sup>226</sup> 356 tion processes. According to Tab. 2, the system reduces 357 concentration from  $4 \times 10 \mu\text{Bq}/\text{m}^3$  to  $<4 \mu\text{Bq}/\text{m}^3$ , repre<sup>341</sup>

V. DISCUSSION senting a reduction of over five orders of magnitude. This 412  $>99.99\%$  removal efficiency was achieved primarily through 360 the synergistic action of the softening resin and the two-stage The system reduces 226 Ra concentration in water from 4 361 RO membranes, with each exhibiting  $>99\%$  Ra removal 414  $\times 105 \mu\text{Bq}/\text{m}^3$  to  $<4 \mu\text{Bq}/\text{m}^3$ , corresponding to a total re<sup>226</sup> 362 efficiency. The Ra removal efficiencies of the main devices 415 duction exceeding five orders of magnitude and an overall 363 used in the UPW system are shown in Tab. 3. The slight vari<sup>416</sup> removal efficiency of  $>99.999\%$ . Even though the RO pro<sup>226</sup> 364 ation in Ra removal efficiency between the two RO stages 417 vides high removal efficiency for particulate matter and ions, 365 is primarily attributable to differences in influent Ra con- 418 a quantitative breakdown of the contributions from individual 366 centration. This system employs two polishing resins in se<sup>419</sup> components (Tab. 3) reveals that the softening resin plays a 367 ries, with tabulated efficiency calculations assuming identical 420 critical and complementary role, accounting for a  $99.88 \pm$  Ra removal performance. 421  $0.04\%$  reduction alone.

Our resin screening revealed sig<sup>369</sup> However, according to the data shown in Tab. 2, mechan- 422 nificant variation in 226 Ra removal efficiency, with cationic 370 ical filtration units (e.g., bag filters, cartridges, multi-media 423 resins demonstrating superior performance over mixed-bed 371 filters) also exhibited incidental Ra removal via adsorp- 424 (anionic/cationic) alternatives. The observed difference is at<sup>2+</sup> 372 tion of Ra onto particulates, enabling concurrent removal 425 tributed to the dominant speciation of 226 Ra as Ra<sup>2+</sup> in low<sup>373</sup> during filtration. Among all devices, only RO integrates both 426 salinity water [31–33], which favors exchange with cationic 374 deionization and particulate removal [34]. 427 functional groups.

This mechanistic understanding guided In addition, the data in Tab. 2 also

indicate that the 226 Ra 428 the selection of a dedicated cationic softening resin over conventional mixed-bed polishing resins. Although the selected Ra rejection (>99%), its pre-377 tank, which is primarily attributable to air ingress through 430 softening resin achieves high 378 tank ventilation valves.

Fiberglass-reinforced plastic tanks 431 RO positioning is mandatory and not interchangeable with 379 require pressure-equalizing vent valves to prevent structural 432 post-RO polishing resin due to substantial organic leaching. 380 damage during water level fluctuations. These valves intro- 433 These leachates cause measurable deterioration of water quality 381 due to ambient air (unfiltered for aboveground tanks, filtered 434 ity, primarily through resistivity reduction. Quantitative water 382 for underground tanks) containing dust-bound Ra progeny 435 quality analysis showed that placing the polishing resin down 383 that dissolve upon water contact. A significant increase in 436 stream of the RO caused resistivity to drop from 18 MΩcm Ra concentration after the pretreatment water tank was 437 to below 1 MΩcm, confirming that organic leachates from 385 traced to sediment introduced during initial commissioning, 438 the resin degrade water quality if placed after the RO and just 386 when sea salt was used for softening resin regeneration. Al- 439 tifying the current upstream configuration. 387 though sea salt was replaced by clean regeneration salt and 440 In reducing the source of 226 Ra pollution, the following 388 the tank was flushed, residual sediment on the tank walls per- 441 two tasks have been identified: 389 sisted as a leaching source. (1) Thorough cleaning of the pretreatment water tank. The 443 periodic regeneration of softening resin, commonly per 444 formed with economical sea salt, was found to introduce sediment 226 445 containing significant Ra contamination. During 390 B.

Relationship between 226 Ra concentration and particulate 446 the initial commissioning phase of the water system, conventional sea salt was used, resulting in a sharp increase in Ra concentration – from 500 μBq/m<sup>3</sup> to 3.0 × 10<sup>5</sup> Tab. 2 also lists the particulate counts and resistivity values 449 μBq/m<sup>3</sup> – after water passed through the pretreatment tank. 393 across the water system. The particulate counts were measured 450 Visual inspection revealed a substantial layer of sediment at 394 using a Battersize C400 optical particle counter (Dan- 451 the tank bottom, which subsequent analysis confirmed originated from Baxter); the small sample volume (20 mL) contributed 452 to the data from the sea salt. The data presented in this paper were 396 to significant data uncertainties. Resistivity was measured using 453 collected after switching to clean regenerant salt and performing 397 an AZ8302 portable conductivity tester (Taiwan Hengxin) 454 ing systematic flushing of the tank. The reduction from 3.0 398 upstream of the secondary RO and a +GF+ Signet 9900 in- 455 × 10 μBq/m to 7.6 × 10 μBq/m confirms the effective 399 line meter downstream. Portable measurements become unreliable 456 ness of replacing the regenerant salt and cleaning the tanks, 400 liable when the resistivity exceeds 10 MΩ\*cm, and the in-line 457 representing an additional 74.7% reduction in post-tank conventional 401 measurements prevent modification

of the sampling point. 458 centration. 402 These constraints resulted in missing high-resistivity data at 459 However, even after adopting clean salt and flushing, resid403 multiple locations. 460 ual sediment remains adhered to the tank walls. This residual The observed correlations between  $^{226}\text{Ra}$  concentration, 461 contamination accounts for the persistent  $^{226}\text{Ra}$  increase of  $\mu\text{Bq}/\text{m}^3$  observed after the pretreatment water 405 particulate counts, and resistivity are a concurrent outcome 462  $7.6 \times 10$  406 of the multi-stage purification process. The softening resin 463 tank. To fully eliminate this source of contamination, a thor $^{226}\text{Ra}$  407 achieves >99% Ra removal by ion exchange ( $\text{Na}^+$  re- 464 ough cleaning of the tank interior is required. As this pro $^{2+}$  408 places Ra ), which minimally influences resistivity and does 465 cedure entails draining the water tank and a temporary sys409 not filter particles due to its 100–500  $\mu\text{m}$  bead size. The si- 466 tem shutdown, it will be scheduled for a suitable maintenance 410 multaneous decrease in all parameters is attributable to their 467 window in the future. (2)Mitigation of contamination from storage tank breather 411 collective removal through successive treatment stages.

$^{226}\text{Ra}$  removal efficiencies of the devices used in the UPW system. When calculating the  $^{226}\text{Ra}$  removal efficiency of the polishing resin, it is assumed that both resin stages have the same efficiency.  $^{226}\text{Ra}$  removal efficiency (%)

Device

Ra concentration before the device ( $\mu\text{Bq}/\text{m}^3$  )

Soften resin

$$4.3 \times 10^5$$

$$99.88 \pm 0.03_{\text{stat}} \pm 0.02_{\text{sys}}$$

$$99.86 \pm 0.04_{\text{stat}} \pm 0.03_{\text{sys}}$$

stage of RO

$$5.5 \times 10^4$$

$$99.47 \pm 0.16_{\text{stat}} \pm 0.13_{\text{sys}}$$

$$1.6 \times 10^4$$

$$42 \pm 27_{\text{stat}} \pm 10_{\text{sys}}$$

$$64.1 \pm 15.1_{\text{stat}} \pm 3.0_{\text{sys}}$$

Polishing resin

valves. Storage tanks introduce measurable radiological con- 494 challenges given the ultra-low concentration target and the tamination primarily through their air-admittance breather 495 large water volume involved. 471 valves.

Comparative measurements at sampling points S9 496 A dedicated 100 t/h UPW production and circulation 472 (upstream of the tank) and S10 (downstream of the tank) show 497 system was developed, integrating multi-stage

purification-473 that the Ra concentration increased from  $(79 \pm 24_{\text{stat}} \pm 498$  including specialized softening resin and RO-with a novel,  $474 \text{ } 9_{\text{sys}}) \mu\text{Bq}/\text{m}$  to  $(15.8 \pm 0.6_{\text{stat}} \pm 2.2_{\text{sys}}) \times 103 \mu\text{Bq}/\text{m}^3$  499 high-sensitivity 226 Ra measurement system ( $3.9 \mu\text{Bq}/\text{m}^3$ ) 475 after passing through the tank, an increase of 200 times. This 500 based on Mn-fiber adsorption and radon emanation. System476 sharp rise confirms that air ingress via the breather valve is the 501 atic characterization across the purification stages revealed 477 dominant contamination mechanism. Two mitigation strate- 502  $>99\%$  removal efficiency for both the softening resin and the 478 gies have been evaluated: installing particulate-retentive fil- 503 two-stage RO. Quantitative analysis further identified regen479 ters on breather assemblies or using boil-off nitrogen as a 504 erant salt impurities and air ingress via tank breather valves 480 clean breathing gas. While nitrogen blanketing could thor- 505 as the two dominant contamination pathways, accounting for 481 oughly eliminate background contamination, it would require 506 the majority of post-purification recontamination.

The JUNO 100 t/h water system successfully reduced 482 a dedicated gas supply system at high cost. Furthermore, the 507 Ra concentration from  $4 \times 105 \mu\text{Bq}/\text{m}^3$  to  $<4 \mu\text{Bq}/\text{m}^3$ , 483 existing boil-off nitrogen capacity at the JUNO site is insuf- 508 484 ficient to meet the system's operational demand. Therefore, 509 achieving a reduction exceeding five orders of magnitude and 485 installing filtration systems at each tank air inlet has been se- 510 surpassing the JUNO requirement by more than an order of This performance establishes a world-leading 486 lected as the practical solution, which will be implemented 511 magnitude. 512 benchmark in ultra-lowRa water purification. 487 during a suitable maintenance period.

Looking forward, the identified contamination pathways 514 provide a clear basis for further optimization. Planned mea515 sures—including thorough cleaning of the pretreatment tank VI. SUMMARY 516 and installation of high-efficiency particulate filters on tank 517 breather valves—are expected to further reduce the JUNO is a multi-purpose neutrino experiment primarily de- 518 concentration in water. More broadly, the high-sensitivity 490 signed to determine the neutrino mass ordering. To ensure 519 measurement system and the key removal components de491 detector safety and minimize background, the CD must be 520 veloped in this work offer a transferable approach for future 492 filled with UPW containing  $<50 \mu\text{Bq}/\text{m}$  of Ra before LS 521 low-background experiments requiring stringent radiopurity 493 introduction—a requirement that presents substantial technical 522 control of large-scale water systems.

[1] F. An, G. An, Q. An et al., Neturino physics with JUNO. 538 J. Phys. G 43, 030401 (2016). <https://doi.org/10.1088/0954-5393899/43/3/030401> [2] A. Abusleme, T. Adam, S. Ahmad et al., JUNO physics 541 and detector. Prog. Part. Nucl. Phys. 123, 103927 (2022). 542 <https://doi.org/10.1016/j.pnpnp.2021.103927> [3] S. Zhang, Y.B. Huang, M. He et al., Sub-GeV events energy 544 reconstruction with 3-inch PMTs in JUNO, Nucl. Sci. Tech. 545 36, 84 (2025). <https://doi.org/10.1007/s41365-025-01678->

- 4 [4] M.H. Liao, K.X. Huang, Y.M. Zhang et al., A ROOT- 547 based detector geometry and event visualization sys- 548 tem for JUNO-TAO. Nucl. Sci. Tech. 36, 39 (2025). 549 <https://doi.org/10.1007/s41365-024-01604-0> [5] C. Cao, J. Xu, M. He et al., Mass production and 551 characterization of 3-inch PMTs for the JUNO exper- 552
- iment. Nucl. Instrum. Meth. A 1005, 165347 (2021). <https://doi.org/10.1016/j.nima.2021.165347>
- [6] A. Abusleme, T. Adam, S. Ahmad et al., Radioactivity control strategy for the JUNO detector. J. High Energy Phys. 2021, 102 (2021). [http://doi.org/10.1007/JHEP11\(2021\)102](http://doi.org/10.1007/JHEP11(2021)102) [7] S. Fukuda, Y. Fukuda, T. Hayakawa et al., The SuperKamiokande Detector, Nucl. Instrum. Meth. A 501, 418-462 (2003). [https://doi.org/10.1016/S0168-9002\(03\)00425-X](https://doi.org/10.1016/S0168-9002(03)00425-X) [8] J. Boger, R.L. Hahn, J.K. Rowley et al., The Sudbury Neutrino Observatory, Nucl. Instrum. Meth. A 449, 172-207 (2000). [https://doi.org/10.1016/S0168-9002\(99\)01469-2](https://doi.org/10.1016/S0168-9002(99)01469-2) [9] T.C. Andersen, I. Blevis, J. Boger et al., Measurement of radium concentration in water with Mn-coated beads at the Sudbury Neutrino Observatory. Nucl. Instrum. Meth. A 501, 399417 (2003). [https://doi.org/10.1016/S0168-9002\(03\)00616-8](https://doi.org/10.1016/S0168-9002(03)00616-8)
- [10] T. Ueno, Radium Concentration Measurements in Super- 602 vatory. Nucl. Instrum. Meth. A 976, 164266 (2020).
- Kamiokande and Search for Magnetic Monopoles 603 <https://doi.org/10.1016/j.nima.2020.164266>
- in Grand Unified Theory, Master' s Thesis at the 604 [22] C. Li, B. Wang, Y. Liu et al., Developing a  $\mu\text{Bq}/\text{m}^3$  University of Tokyo (2021). [https://www-sk.icrr.u-](https://www-sk.icrr.u-tokyo.ac.jp/assets/paper/list/pdf/mthesis/2008/master606) 605 level 226 Ra concentration in water measurement system [tokyo.ac.jp/assets/paper/list/pdf/mthesis/2008/master606](https://www-sk.icrr.u-tokyo.ac.jp/assets/paper/list/pdf/mthesis/2008/master606) for the Jiangmen Underground Neutrino Observatory. Nucl. ueno.pdf Instrum. Meth. A 1063, 169257 (2024). [https://doi.org/](https://doi.org/10.1016/j.nima.2024.169257) 559 [11] Electronic Grade Ultra- pure Water, SJ/T 11452-2013 (2013). 608 [10.1016/j.nima.2024.169257](https://doi.org/10.1016/j.nima.2024.169257) <https://std.samr.gov.cn/> 609 [23] China National Standards Full-Text Disclosure System. 561 [12] M.
- Tawalbeh, L. Qalyoubi, A.Al-Othman et al., In- 610 <https://openstd.samr.gov.cn>
- sights on the development of enhanced antifouling re- 611 [24] J.X. Wang, T.C. Andersen, J.J. Simpson, An electro563 verse osmosis membranes: Industrial applications and chal- 612 static radon detector designed for water radioactivity mea564 lenges. Desalination 553, 116460 (2023). [https://doi.org/](https://doi.org/10.1016/j.desal.2023.116460) 613 surements. Nucl. Instrum. Meth. A 421, 601-609 (1999). [10.1016/j.desal.2023.116460](https://doi.org/10.1016/j.desal.2023.116460) [https://doi.org/10.1016/S0168-9002\(98\)01230-3](https://doi.org/10.1016/S0168-9002(98)01230-3) 566 [13] Z.U. Khan, M. Moronshing, M. Shestakova et al., Electro- 615 [25] Y.Y. Chen, Y.P. Zhang, Y. Liu et al., A study on the radon deionization (EDI) technology for enhanced water treatment 616 removal performance of low background activated carbon. and desalination: A review. Desalination 548, 116254 (2023). 617 J. Instrum. 17, P02003 (2022). <https://doi.org/10.1088/1748569> <https://doi.org/10.1016/j.desal.2022.116254> 0221/17/02/P02003 570 [14] B. Wang, C. Guo, Y.G. Xie et al., Measurement of 619 [26] C. Guo, J.C. Liu, Y.P. Zhang et al., Study on the radon re571 the radon concentration in the ultrapure

water of the 620 mval for the water system of Jiangmen Underground Neutrino JUNO-LS UPW system. *J. Instrum.* 20, P03028 (2025). 621 Observatory. *Radiat. Detect. Technol. Methods* 2, 48 (2018). <https://doi.org/10.1088/1748-0221/20/03/P03028> <https://doi.org/10.1007/s41605-018-0077-8> 574 [15] Y. Nakano, T. Hokama, M. Matsubaara et al., Measurement 623 [27] Y. Liu, Y.P. Zhang, J.C. Liu et al., System upgrade of the radon concentration in purified water in the Super- 624 for  $\mu\text{Bq}/\text{m}^3$  level 222 Rn concentration measurement. *J.*

Kamiokande IV detector. *Nucl. Instrum. Meth. A* 977, 164297 625 *Instrum.* 18, T03002 (2023). <https://doi.org/10.1088/1748577> (2020). <https://doi.org/10.1016/j.nima.2020.164297> 0221/18/03/T03002 578 [16] T.Y. Guan, Y. P. Zhang, B. Wang et al., Development of low- 627 [28] C. Li, Y. Zhang, L. Lv et al., Study on the radon radon ultra-pure water for the Jiangmen Underground Neutrino 628 adsorption capability of low-background activated car580 Observatory. *Nucl. Instrum. Meth. A* 1063, 169244 (2024). 629 bon. *J. Radioanal. Nucl. Chem.* 333, 337-346 (2024). <https://doi.org/10.1016/j.nima.2024.169244> <https://doi.org/10.1007/s10967-023-09211-w> 582 [17] G.R. Araujo, L. Baudis, Y. Biondi et al., The upgraded 631 [29] Y. Nakano, H. Sekiya, S. Tasaka et al., Measurement low-background germanium counting facility Gator for high- 632 of radon concentration in super-Kamiokande' s buffer sensitivity  $\gamma$ -ray spectrometry. *J. Instrum.* 17, P08010 (2022). 633 gas. *Nucl. Instrum. Meth. A* 867, 108-114 (2017). <https://doi.org/10.1088/1748-0221/17/08/P08010> <https://doi.org/10.1016/j.nima.2017.04.037> 586 [18] S. Ito, Y. Takaku, M. Ikeda et al., Determination of trace 635 [30] Y. Nakano, T. Hokama, M. Matsubara et al., Measurement level thorium and uranium in high purity gadolinium sulfate 636 of the radon concentration in purified water in the Super588 using ICP-MS with solid-phase chromatographic extraction 637 Kamiokande IV detector. *Nucl. Instrum. Meth. A* 977, 164297 resins. *AIP Cong. Proc.* 1921, 030003 (2018). <https://doi.org/10.1016/j.nima.2020.164297> 10.1063/1.5018990 639 [31] B.L.

Dickson, The environmental behavior of ra591 [19] W.S.

Moore and D.F. Reid, Extraction of radium 640 dium. IAEA. Vol. 1. No. 310. 335-372 (1990). from natural waters using manganese-impregnated 641 <https://inis.iaea.org/records/swprd-wbq70> acrylic fibers. *J. Geophys. Res.* 78, 8880-8886 (1973). 642 [32] D. Porcelli and P.W. Swarzenski, The Behavior of U- and Th594 <https://doi.org/10.1029/JC078i036p08880> series Nuclides in Groundwater. *Rev. Mineral. Geochem.* 52, 595 [20] R.N. Peterson, W.C. Burnett, N. Dimova et al., Com- 644 317-361 (2003). <https://doi.org/10.2113/0520317> parison of measurement methods for radium-226 on 645 [33] F. Carvalho, D. Chambers, S. Fernandes et al., The Environ597 manganese-fiber. *Limnol. Oceanogr. Methods* 7, 196-205 646 mental Behaviour of Radium: Revised Edition. IAEA Techni598 (2009). <https://doi.org/10.4319/lom.2009.7.196> cal Reports Series No. 476 (2014). <http://www.iaea.org/books> 599 [21] L.F. Xie, J.C. Liu, S.K. Qiu et al., Developing the ra- 648 [34] PURETEC Industrial

Waterm, The Basics - Reverse Osmosis. dium measurement system for the  
water Cherenkov de- 649 <https://puretecwater.com> tector of the Jiangmen  
Underground Neutrino Obser553

*Note: Figure translations are in progress. See original paper for figures.*

*Source: ChinaXiv –Machine translation. Verify with original.*